Atmos. Meas. Tech. Discuss., 8, 11953–11986, 2015
www.atmos-meas-tech-discuss.net/8/11953/2015/
doi:10.5194/amtd-8-11953-2015

Atmospheric Measurement Techniques Discussions

Ground-based remote sensing scheme for monitoring aerosol–cloud interactions

K. Sarna and H. W. J. Russchenberg

TU Delft Climate Institute, Faculty of Civil Engineering and Geotechnology, Delft University of Technology, Stevinweg 1, 2628 CN, Delft, the Netherlands

Received: 13 October 2015 – Accepted: 4 November 2015 – Published: 17 November 2015

Correspondence to: K. Sarna (k.sarna@tudelft.nl)

Published by Copernicus Publications on behalf of the European Geosciences Union.

Abstract

A method for continuous observation of aerosol–cloud interactions with ground-based remote sensing instruments is presented. The main goal of this method is to enable the monitoring of cloud microphysical changes due to the changing aerosol concentration. We use high resolution measurements from lidar, radar and radiometer which allow to collect and compare data continuously. This method is based on a standardised data format from Cloudnet and can be implemented at any observatory where the Cloudnet data set is available. Two example study cases were chosen from the Atmospheric Radiation Measurement (ARM) Program deployment at Graciosa Island, Azores, Portugal in 2009 to present the method. We show the Pearson Product–Moment Correlation Coefficient, r, and the Coefficient of Determination, r^2 for data divided into bins of LWP, each of $10\,\mathrm{g\,m^{-2}}$. We explain why the commonly used way of quantity aerosol cloud interactions by use of an ACI index ($\mathrm{ACI}_{r,\tau} = \mathrm{d}\ln r_\mathrm{e}, \tau / \mathrm{d}\ln\alpha$) is not the best way of quantifying aerosol–cloud interactions.

1 Introduction

Low-level water clouds are considered one of the main sources of uncertainties in climate change predictions. According to the Fifth Assessment Report (AR5) of the Intergovernmental Panel on Climate Change (IPCC, 2014), clouds and the effects of aerosol on their macro- and micro-structure continue to contribute to the largest uncertainty in the estimation and interpretation of the Earth's energy budget. Low-level clouds impact mainly the shortwave radiation budget as it is mostly sensitive to the cloud albedo. The effect of aerosol concentration on cloud reflectance is often referred to as the Twomey effect (Twomey, 1974), albedo effect or first indirect effect. It is based on the close relation between the aerosol concentration below the cloud and the droplet concentration of a cloud formed above.

AMTD
8, 11953–11986, 2015

An ample number of studies have been made in order to quantify the impact of aerosol–cloud interactions (McComiskey and Feingold, 2012). Some observational studies of the aerosol effect on clouds used either surface remote sensing instruments at specific locations (e.g., Feingold, 2003) or processed airborne data from short lived field campaigns (e.g., Twohy et al., 2005; Lu et al., 2008). Other studies rely on a combination of both surface remote sensing and aircraft in-situ observations (e.g., Garrett et al., 2004; Kim et al., 2008; McComiskey et al., 2009). Many approaches used satellite remote sensing to characterise the aerosol effect on a global scale (e.g., Kaufman et al., 2005). The broad scope of different methods and scales used makes it difficult to quantitatively compare results from these different studies. For that reason the impact of an increasing aerosol concentration on cloud microphysical properties remains debatable and therefore is the main focus of this study.

We present an approach for monitoring interactions between aerosol and clouds with ground-based remote sensing instruments. We use specifically zenith-pointing cloud radar, lidar and microwave radiometer to characterise cloud microphysical properties and the aerosol concentration in the same column. Thanks to the unique capabilities of the ground-based remote sensors data can be collected and compared continuously. Further, because we use the upward pointing ground-based instruments we are able to observe the aerosol activation process exactly where it happens – below the cloud, in the cloud base region. Due to the fine spatial and time resolution available there is no separation in time or space between measured cloud and aerosol properties. We developed the monitoring scheme on the basis of the standardised data format from Cloudnet (Illingworth et al., 2007). The method described here can be implemented on multiple ground-based observational sites (e.g., the European ACTRIS network – Aerosol, Clouds and Trace gases Research InfraStructure and the US Atmospheric Radiation Measurement (ARM) Program – both databases provide Cloudnet dataset), where a long term database of measurements already exists so that statistical calculations of aerosol and cloud interactions for different locations can be performed.

AMTD
8, 11953–11986, 2015

The structure of this paper is following: first, we provide a description of the methodology for estimating the relationship between the aerosol concentration below the cloud base and the cloud droplet concentration and the droplet sizes in the cloud base region, as well as the combination of instruments and proxies used for the method. Then we show two example study cases from the ARM Mobile Facility at Graciosa Island at the Azores, Portugal. Finally, we discuss the possibilities of implementing this method over the network of cloud profiling observatories in Europe.

2 Quantifying interactions between aerosol and cloud

Very often in the literature the term aerosol–cloud interactions is associated with quantification of the impact of aerosol on cloud albedo. This relation was first postulated by Twomey (1974). Through experimental studies he showed that the number concentration of aerosol (N_a) below the cloud is monotonically related to the cloud droplet number concentration (N_d):

$$N_d \propto N_a^{\gamma}, \tag{1}$$

(Twomey and Warner, 1967). The aerosol number concentration and cloud droplet concentration are not directly proportional because the increased concentration of aerosol that can be activated into cloud droplets can lead to lowering of the maximum relative humidity that can be reached in the cloud base region. The value of γ varies between 0.7 and 0.8 between different experimental studies (Pruppacher and Klett, 2010; Twomey, 1974). Twomey (1977) further derived a theoretical relationship between the aerosol concentration and cloud albedo. He proposed that, since an increased aerosol concentration results in an increased number of cloud condensation nuclei (CCN) for cloud droplet formation, it will also lead to an increased cloud droplet concentration. If the amount of available water for the cloud formation is constant, by assuming a constant value of liquid water path (LWP), the increased cloud droplet concentration will

AMTD
8, 11953–11986, 2015

mean that the effective radius of cloud droplets (r_e) is smaller. As the cloud droplet concentration and cloud effective radius influence the value of the cloud optical thickness (τ_d) it can be assumed that the optical thickness will be rising with the increase of the droplet concentration,

$$\tau_d \propto N_d^{1/3} \tag{2}$$

(Twomey, 1974), and the decrease of the droplet radius:

$$r_e \propto \frac{\mathrm{LWP}}{\tau_d}, \tag{3}$$

(Stephens, 1978).

Theoretical relationships between variables in Eqs. (1)–(3) led to the formulation of a relation between the aerosol optical thickness (τ_a), as τ_a is a function of the aerosol number concentration (N_a), and the effective radius of cloud droplets (r_e):

$$r_e \propto \tau_a^{-\gamma/3}, \tag{4}$$

which is a basic theoretical relation used presently to quantify the effect described by Twomey. In order to empirically quantify the interactions between aerosol and cloud Feingold et al. (2001) introduced the indirect effect index (IE), later referred to as the ACI (Aerosol–Cloud Interactions),

$$\mathrm{IE} = \mathrm{ACI}_{r/\tau} = \left.\frac{\mathrm{d}\ln r_e/\tau_d}{\mathrm{d}\ln \alpha}\right|_{\mathrm{LWP}} \quad 0 < \mathrm{ACI}_{r/\tau} < 0.33, \tag{5}$$

where α is an observed proxy of the amount of aerosol and varies between studies. It can include parameters such as aerosol number concentration (N_a), aerosol optical thickness (τ_a) or Aerosol Index (AI), which is a product of τ_a and Angström exponent.

AMTD
8, 11953–11986, 2015

It is important to note that in order to derive Eq. (2) Twomey made a series of assumptions. He restricted his analysis to homogeneous clouds with a thin optical thickness where cloud droplet number concentration and aerosol optical thickness can be considered directly proportional to an increasing pollution. The assumption about aerosol optical thickness meant that he considered all components in the aerosol to increase together and at the same proportion. Further, he assumed that absorption is not greatly modified when the cloud forms and therefore the increase in the cloud nuclei concentration is proportional to the absorption optical thickness of the aerosol. The combination of these assumptions greatly minimises the amount of observational study cases where the relation from Eq. (2) can be applied. Another important, and often omitted, factor is that the cloud droplet concentration (N_d) is modified by mixing, collision and coalescence, evaporation and coagulation within the cloud. However, at the area close to the cloud base, where the cloud is at the early formation stage, the initial N_d is determined by the amount of nuclei able to activate into cloud droplets at or below the maximum supersaturation in the cloudy air (Twomey and Warner, 1967). This means that the number concentration of aerosol to the number concentration of cloud droplets should be related below the cloud base. Cloud droplet concentration can be related with the cloud reflectance and albedo only under an assumption that the cloud is homogeneous and its properties do not change from the cloud base to the cloud top. The relation from the Eq. (5) is derived from the cloud reflectance and under all the above mentioned assumptions its transition to other parameters and actual observations is not straightforward.

In this study we focus on the aerosol–cloud interactions as an approximation of the nucleation process without relating it to the cloud albedo. We design a method that enables monitoring daily the microphysical process between aerosol and clouds. To avoid the ambiguity of the ACI empirical form (Eq. 5), we quantify the relation between cloud and aerosol properties with statistical parameters making only the assumption that the aerosol number concentration in the cloud base region is monotonically related to the cloud droplet concentration (Eq. 1) and that the increase of the cloud droplet concen-

AMTD
8, 11953–11986, 2015

tration leads to a decrease of the cloud droplet size. We use the Pearson Product–Moment Correlation Coefficient, r, to establish how dependent the cloud drop size is on the aerosol concentration. The sign of the correlation coefficient will show if the increasing concentration of aerosol actually decreases the cloud droplet size. We also calculate the Coefficient of Determination, r^2, which will suggest the percentage of the variability in cloud droplet size that can be explained by changes in aerosol concentration. We want to analyse data daily when the specific conditions are present (see Sect. 3.3) and divide data into small bins of Liquid Water Path (LWP) to approximate the conditions in each bin to a constant LWP, as postulated by Twomey. Due to daily data analysis we will always have a smaller sample than in the case of data aggregated from a longer periods. For that reason we also perform student's t test for every considered LWP bin to establish if data is statistically significant. The Correlation Coefficient, r, can determine how strong is the relation between the aerosol and cloud properties and the Coefficient of Determination, r^2, gives information about the amount of the variability in cloud properties that can be explained by changes in aerosol properties.

3 Methodology

3.1 Instrumentation and data

The goal of our method is to monitor the interactions between aerosol and clouds. We combine measurements from three separate instruments, cloud radar, ceilometer and microwave radiometer, to capture and monitor the influence of a changing aerosol concentration on the cloud microphysical properties. Very often collocated measurements of aerosol and cloud properties are not available at a similar time scale or are being collected only during specific measurements campaigns. To gain a better understanding of the aerosol impact on cloud microphysical properties we need to have continuous measurements over multiple locations. Further, to eliminate rapid variation in the meteorological conditions we want to evaluate data daily. Both those requirements can only

AMTD
8, 11953–11986, 2015

be satisfied by ground-based remote sensing instruments which are at the core of this monitoring scheme.

As a microphysical process, aerosol–cloud interactions should be observed in the same air column, at a high temporal resolution. We used the Cloudnet dataset, which provides a set of high quality measurements from radar, lidar and a microwave radiometer (Hogan and O'Connor, 2004). Additionally, each pixel of the data set is categorised in terms of the presence of liquid droplets (cloud, rain or drizzle), ice, insects or aerosol. This categorisation allows us to construct an algorithm that can be applied to specific targets only.

3.2 Aerosol and cloud properties proxies

Clouds are formed when aerosol particles are activated into cloud droplets. Activation is a change from stable to unstable growth due to the increase of the ambient humidity. Haze droplets grow through the peak of the Köhler curve (Köhler, 1936) and are transformed into cloud droplets. When a higher concentration of the aerosol particles is present, the competition for the excess water vapour will be greater and thus, the resulting cloud droplets will be smaller (Lamb and Verlinde, 2011).

In low level liquid water clouds, in particular Stratocumulus, the number of the activated droplets is approaching the concentration of the aerosol accumulation mode (particles between 0.1 and 1 µm), making that concentration itself the primary determinant of the cloud droplet concentration (e.g., Martin et al., 1994; Lu et al., 2007). Based on an adiabatic cloud parcel model representing the hygroscopic growth of CCN and droplet condensation, Feingold (2003) concluded that aerosol number concentration (N_a) contributes most significantly to aerosol effects on clouds. Other aerosol parameters, such as size, breadth of the aerosol size distribution and its chemical composition are of a secondary importance.

AMTD
8, 11953–11986, 2015

3.2.1 Aerosol number concentration

Numerous proxies have been used in the past to represent the aerosol concentration. In this method we aim at using continuous measurements with a high spatial and temporal resolution. Such dataset is available from a ceilometer. Several research indicate that a ceilometer can be used as a quantitative aerosol measurement instrument (Sundström et al., 2009; Wiegner et al., 2014). Backscatter from ceilometer (β) can be approximated to:

$$\beta \approx \int_0^\infty N_a(D_a) D_a^2 \mathrm{d}D_a, \tag{6}$$

where N_a is the number concentration of aerosol and D_a is the aerosol diameter. The averaged β shows good correlations with the in situ measurements of the mass concentration of the particulate matter up to 10 µm (PM_{10}) and smaller than 2.5 µm ($PM_{2.5}$) (Münkel et al., 2006).

In this method we use an integrated value of the ATB in order to represent the whole column of aerosol below the cloud. We only consider well-mixed conditions (Sect. 3.3). Data is integrated from the level of a complete overlap (minimum height where the cross-section of the lidar laser beam is completely in the field of view of the receiver's telescope Kovalev, 2015) up to 300 m below the cloud base. The distance from the cloud minimises the amount of cloud and haze droplets or wet aerosol mixed through the considered aerosol background. Previous studies often used a set height of the aerosol proxy (e.g. Raman lidar extinction at 350 m Feingold et al., 2006). We found that by considering the level of aerosol proxy and cloud at a set distance from the cloud base the dependence of cloud properties on aerosol concentration is bigger. Therefore we use a height for comparison that is based on a set distance from the cloud base.

Note that Cloudnet ceilometers are calibrated in accordance with the O'Connor et al. (2004) method which introduces the calibration uncertainty of up to 10 %. The precision

AMTD
8, 11953–11986, 2015

of the measurements is difficult to estimate as the internal processing algorithms are proprietary. A single value of 0.5 dB is used for all pixels (Hogan and O'Connor, 2004).

3.2.2 Cloud droplets size and number concentration

Aerosol–cloud interactions are described as the response of the microphysical properties of the cloud to the change of the aerosol number concentration. The cloud properties that we are specifically interested in are the cloud droplet size and the number concentration of the droplets. Both these variables are obtained through a retrieval of cloud microphysical properties from measurements.

For retrieval of the cloud droplet concentration (N_d) and the cloud droplet effective radius (r_e) from cloud radar and MWR observations we apply a method according to Frisch et al. (2002). Assuming that N_d and gamma cloud droplet distribution with a fixed distribution shape (ν) are constant with height, the r_e can be derived from the Radar Reflectivity Factor (Z) and the MWR retrieved LWP:

$$r_e(h) = \left(\frac{(\nu+2)^3}{(\nu+3)(\nu+4)(\nu+5)}\right)^{\frac{1}{3}} \left(\frac{\pi\rho_w \sum_{i=1}^{n} Z^{\frac{1}{2}}(h_i)\Delta h}{48\mathrm{LWP}}\right)^{\frac{1}{3}} Z^{\frac{1}{6}}(h), \quad (7)$$

where ρ_w is the density of liquid water ($10^6\,\mathrm{gm}^{-3}$), Δh is the the length of the radar range gate, $Z(h_i)$ is the reflectivity factor at the ith radar measured gate and n represents the number of the in-cloud radar-measured gates. The cloud droplet number concentration (N_d) is calculated from the following formula:

$$N_d = \left(\frac{(\nu+3)(\nu+4)(\nu+5)}{\nu(\nu+1)(\nu+2)}\right)\left(\frac{6\mathrm{LWP}}{\pi\rho_w \sum_{i=1}^{n} Z^{\frac{1}{2}}(h_i)\Delta h}\right). \quad (8)$$

Both of those retrieved properties have been evaluated against other methods in Knist (2014). The comparison of different retrieved microphysical cloud properties reveals

AMTD
8, 11953–11986, 2015

that r_e is the most robust parameter. The estimated uncertainties in r_e are about 10–15 % and in N_d around 40–60 %. In both proxies the uncertainties are due to observational errors and algorithm assumptions. Following Knist (2014), the gamma cloud droplet distribution shape parameter is set to 8.7. This value is obtained from the ratio between the third and second moment of the droplet distribution and has been found in reanalysis of the in-situ observations of Stratocumulus clouds (Brenguier et al., 2011).

Similarly to the aerosol proxy, we compare the r_e at a set distance from the cloud base. We set this distance at 85 m above the cloud base detected from the lidar measurements, as the lidar can detect the cloud base height more precisely than the radar. The distance of 85 m ensures that the cloud is detected by both instruments.

3.2.3 Relation between aerosol and cloud proxies

The strong relation between aerosol concentration and cloud droplet concentration (Eq. 1) is postulated both by theory and observations. We expect to see an inverse relationship between the aerosol concentration and cloud droplets size. With the increase of the aerosol concentration, the cloud droplet size is expected to decrease while at the same time the cloud droplet concentration is expected to increase.

Applying those relations to the proxies of cloud and aerosols we use in this method we should observe a decrease of the cloud droplet effective radius (r_e) with the increase of the integrated attenuated backscatter (ATB). The cloud droplet number concentration (N_d) should be increasing with the increasing value of the integrated attenuated backscatter (ATB).

3.3 Data selection criteria

Clouds are complicated systems with many processes taking place at the same time. Hence, singling out a small microphysical process is difficult. Analysed data need to be limited by implementing a number of filters. Firstly, this monitoring scheme applies only to liquid water clouds on top of the boundary layer in well-mixed conditions. This

AMTD
8, 11953–11986, 2015

limitation ensures that the cloud is not decoupled from the boundary layer and the aerosol background below the cloud (Feingold et al., 2006). Secondly, we can only consider data when no precipitation is present, including drizzle, as it can obscure the formative stage of a cloud (Feingold et al., 2003). We use the Cloudnet categorisation data for the classification of the observed targets. Thirdly, only data with a changing aerosol background is analysed. The assumption of aerosol–cloud interactions is that the variation in the aerosol concentration affects the variation in the cloud properties. Thus, both aerosol and cloud parameters need to vary to observe the impact of aerosol on cloud. This scheme relies on measurements from three separate instruments. Only profiles where all three instruments provide good quality data can be analysed.

Some larger scale factors, such as boundary layer dynamics or variations in temperature, pressure or humidity, can influence changes in the cloud. We ensure similar meteorological conditions by analysing aerosol and cloud properties on a daily basis. This minimises the influence of variations in general weather conditions. To further minimise the impact of these factors on the calculation of aerosol–cloud interactions, due to some daily variations, we apply a constraint on LWP. It's prime role is to isolate the aerosol activation process from different interactions that can happen at the same time. Daily datasets are divided into profiles where the value of LWP is similar. We divide the data into bins of LWP of $10\,g\,m^{-2}$, as creating smaller bins is difficult due to the limited data points. LWP should be above $30\,g\,m^{-2}$ and below $150\,g\,m^{-2}$. Values below $30\,g\,m^{-2}$ are disregarded because of the uncertainty of LWP calculated from MWR, which is around $15\,g\,m^{-2}$ (Turner et al., 2007). The values above $150\,g\,m^{-2}$ are excluded to avoid precipitating clouds.

The analysis of an aggregated dataset grouped by varying meteorological regimes would be a good way of getting a better understanding of aerosol–cloud interactions drivers. Such a study can be made with the method presented here but is beyond the scope of this manuscript.

AMTD
8, 11953–11986, 2015

4 Application of the method to observations from Graciosa Island, Azores

We present here two example study cases for the practical application. The deployment of the Atmospheric Radiation Measurement Program (ARM) Mobile Facility at Graciosa Island, Azores in 2009 and 2010 provides a comprehensive data set for assessing aerosol effects on liquid water clouds. Boundary layer clouds were the most frequently observed cloud type (40–50 %) with the maximum occurrence during the summer and fall months under the presence of anticyclonic conditions (Rémillard et al., 2012). The instruments we use in this study are a W band ARM (95 GHz) Cloud Radar (WACR) (Widener, 2004), a laser ceilometer (Vaisala CT25K) and a two-channel microwave radiometer (MWR). Data from this campaign is available in the standardised Cloudnet format, which is the basis of calculations presented here. The Cloudnet data set is re-gridded to the vertical resolution of the radar (42.86 m) and the time resolution of the radiometer (30 s). Table 1 summarises all measurements and all products derived for the data analysis.

Based on the data selection criteria presented in the section above we identified 2 study cases for testing the method: 3 November 2009 and 29 November 2009. Both cases showed small variability of the LWP which enabled distribution of data into small bins of LWP $\mathrm{g\,m^{-2}}$. The station was located at the North-East shore of the island, situated upwind in order to reduce the impact of the island. The NOAA HYSPLIT back trajectory model (Draxler et al., 1997) indicated that the aerosol for the selected days were coming from marine sources. This single source of aerosol allows us to test the method without adding the extra complexity of a multiple aerosol sources background.

4.1 Study case from 3 November 2009

The conditions on 3 November 2009 were characterised by a northerly wind of about $2.5\,\mathrm{m\,s^{-1}}$ in the boundary layer. The cloud cover was persisting the whole day, with periods of drizzle and heavy rain after 18:00 UTC. Precipitation-free periods were identified between 00:00 and 05:00 UTC, with a second short period between 13:30 and

AMTD
8, 11953–11986, 2015

15:00 UTC, set after a light precipitation event (Fig. 1). Based on the Cloudnet categorisation and the measurements from WACR and MWR, only data in these 2 periods were analysed on that day. LWPs in the selected periods ranged from 15 to 130 g m^{-2}. As few data points were available with LWP above 110 g m^{-2}, we limit the data analysed to a LWP between 30 and 110 g m^{-2}. The cloud base was located around 800 m above ground level (a.g.l.) between 00:00 and 05:00 UTC and around 500 m a.g.l. between 13:30 and 15:00 UTC.

Figure 2 presents the time-height cross section of the retrieved microphysical cloud properties. Only data from time steps meeting the data selection criteria are calculated. In the chosen periods r_e varies from 2 to 12 µm, with a mean radius 5 µm and a standard deviation of 1.6 µm. N_d ranges in the selected periods from 200 to 1600 cm^{-3}. Some values are much higher than the observational data for Stratocumulus. N_d rarely exceeds 500 cm^{-3} and is generally lower (200 to 300 cm^{-3}) for marine Stratocumulus (Martin et al., 1994).

Aerosol background (represented by ATB) in the selected periods is variable with the mean value 0.82×10^{-3} sr^{-1} and a standard deviation of 0.31×10^{-3} sr^{-1}. ATB in the period between 13:30 and 15:00 UTC is significantly lower, mainly because it was followed by a period of precipitation and the cloud base was located considerably lower than in the first period.

All data points available on 3 November 2009 are divided into bins based on the value of the LWP which ranges from 30 to 110 g m^{-2}. Data was divided into 8 separate bins, each covering 10 g m^{-2}. Figure 5 presents relation between the integrated attenuated backscatter ATB and cloud droplet effective radius r_e together with the Pearson Product–Moment Correlation Coefficient, r, and the Coefficient of Determination, r^2 corresponding to each bin.

The coefficient of determination, r^2, suggests the percentage of the variability in cloud droplet size that can be explained by changes in aerosol concentrations. For example, for the LWP values between 40 and 50 g m^{-2} 65 % of the variability in the r_e can be explained by the changes in the aerosol concentration, represented by ATB.

AMTD
8, 11953–11986, 2015

Note that those values are quite high for 3 November 2009 in the LWP range from 30 to 70 g m^{-2} and get lower for the higher LWP values. This may indicate that aerosol–cloud interactions representing the activation process are more significant only for the lower LWP values and for the higher values of LWP other processes, such as collision and coalescence of cloud droplets or cloud top cooling, may play a more important role. Another possible explanation can be the presence of drizzle when LWP is above 70 g m^{-2}. Some studies suggest that marine Stratocumulus clouds can form drizzle particles at LWP values as low as 75 to 100 g m^{-2} (Rémillard et al., 2012).

Figure 7 shows the relation between the integrated attenuated backscatter, ATB, and the cloud droplet number concentration, N_d, together with the corresponding Pearson Product–Moment Correlation Coefficient, r, and the Coefficient of Determination, r^2. Cloud droplet number concentration increases with the increase of aerosol concentration (represented by ATB) as expected by the aerosol–cloud interactions. Based on the coefficient of determination, r^2, around 33 % of the variation in the cloud droplet concentration can be attributed to the changes in the aerosol background.

4.2 Study case from 29 November 2009

On 29 November 2009 a northerly wind of about 2 m s^{-1} in the boundary layer persisted most of the day. Periods of drizzle and rain were occurring throughout the day, with a heavy precipitation after 15:00 UTC. Therefore we only consider data before 14:00 UTC.

The cloud base was located around 1600 m a.g.l. (Fig. 3). Periods between 00:00 to 03:00, 05:30 to 06:00 and 08:30 to 14:00 UTC correspond with the data selection criteria. In all cases, the categorisation provided by Cloudnet identifies that the cloud layer consists of liquid water cloud and aerosol only. LWP in the selected periods varies between 15 and 150 g m^{-2}. As there are few data points available with LWP above 90 g m^{-2} we limit the data analysed to a LWP between 30 and 90 g m^{-2}.

Figure 4 shows the retrieved properties in periods corresponding to our data selection criteria. In the selected periods N_d varies from 200 to 1700 cm^{-3}, with a stan-

AMTD
8, 11953–11986, 2015

dard deviation of 230 cm^{-3} and mean value of 550 cm^{-3}. Note that values of N_d over 2500 cm^{-3} (around 02:00 UTC) were excluded from the analysis. Values of r_e range between 2.5 and 7.5 µm, with a mean radius 4.7 µm and a standard deviation of 0.95 µm. ATB in the selected period has a mean value of 1.4×10^{-3} sr^{-1} and a standard deviation of 0.25×10^{-3} sr^{-1}. It should be noted that on 29 November ATB is higher, but, even accounting for the uncertainty of ATB, the variation is smaller than on 3 November.

Suitable data from 29 November 2009 are divided into bins based on the value of the LWP which ranges from 30 to 90 $g\,m^{-2}$. Data was divided into 6 separate bins, each covering 10 $g\,m^{-2}$. Figure 6 presents relation between the integrated attenuated backscatter ATB and cloud droplet effective radius r_e together with the Pearson Product–Moment Correlation Coefficient, r, and the Coefficient of Determination, r^2, corresponding to each bin.

Examination of the correlation coefficient, r, and the coefficient of determination, r^2 reveals that on average both of these statistical values are lower on 29 November than on 3 November, even though the total number of observations is higher on that day. The possible explanation for this is that the cloud base was more than 1500 m a.g.l.. This may suggest that the impact of the aerosol background below the cloud is smaller. Also, as we indicated before, the variation in the aerosol background is smaller. If the aerosol background below the cloud is more stable separating cloud microphysical process within the cloud might be more difficult. Also, it was indicated by Feingold (2003) that other aerosol parameters than N_a, such as the size distribution and composition, are of a greater importance when the aerosol loading is higher. Note that for the case from 29 November 2009 the correlation coefficient for the LWP bin from 80 to 90 $g\,m^{-2}$ is actually positive. This suggest that at this LWP cloud droplets grow through different process, such as collision and coalescence, and the activation of aerosol into cloud droplets is a secondary process.

Figure 8 presents the relation between the integrated attenuated backscatter, ATB, and the cloud droplet number concentration, N_d, together with the corresponding Pearson Product–Moment Correlation Coefficient, r, and the Coefficient of Determination,

AMTD
8, 11953–11986, 2015

r^2. Again it can be clearly observed that the cloud droplet number concentration increases with the increase of aerosol concentration (represented by ATB). Data from 29 November shows less scatter than on 3 November, but the correlation coefficient is lower.

4.3 Comparison of example study cases

Table 2 summarises statistical parameters, including the number of observations within each LWP bin, for both study cases presented here. Values of the correlation coefficient r are generally higher for the value of LWP in the range from 30 to 70 g m^{-2}. This suggest that aerosol–cloud interactions connected to the droplet activation play a more important role in the lower values of LWP and that supposedly drizzle can obscure the process of the activation of aerosol into cloud droplets.

As we mentioned before, due to using daily data it is necessary to check if the sample in each bin can give a representative value of the correlation coefficient. In order to test that we use a student's p test. For all bins on 29 November and bins of LWP between 30 and 80 g m^{-2} on 3 November presented correlations are significant at 99 % level. For the bins between 90 and 100 LWP on 3 November presented correlations are significant at 95 % probability level. For the last bin (between 100 and 110 LWP) the correlations are only significant at 90 % probability level due to a very small sample size.

5 Summary and outlook

In this paper we present a method for observing interactions between aerosol and clouds. This method enables continuous monitoring of cloud microphysical responses to the changing aerosol background through a use of high resolution ground-based remote sensing instruments. This scheme is developed on the base of a standardised data format from Cloudnet. We used the Cloudnet cloud categorisation product to

AMTD
8, 11953–11986, 2015

choose data points with the specific targets only (liquid water clouds and aerosols) and instead of aggregating data with same values of LWP over a longer period we process data from every day separately.

Daily data for analysis is selected based on a range of criteria. Data points complying with all of them are divided into bins of LWP where each bin is $10\,g\,m^{-2}$. For every bin we calculate statistical parameters such as the Pearson Product–Moment Correlation Coefficient, r, and the Coefficient of Determination, r^2. In order to test the statistical significance of every bin sample we perform a student's t test. We explained that the use of an $ACI_{r,\tau}$ estimation as commonly used in similar studies is not the best way of quantifying aerosol–cloud interactions. We show that the statistical parameters can be representative of the dependence of the cloud droplet size on the aerosol concentration. With the use of the Coefficient of Determination, r^2, we can determine the percentage of variability in the drop size that can be attributed to aerosol concentration. It is important to only use statistical information when data is analysed on a daily basis to ensure no big variation in the meteorological conditions. Collocation of daily data into larger datasets can be made, but should be based on very similar meteorological conditions.

We showed two example case studies to present this method. Both datasets come from the deployment of the Atmospheric Radiation Measurement Program (ARM) Mobile Facility at Graciosa Island, Azores in 2009 and 2010. The presented cases both are characterised by a marine Stratocumulus clouds, both come from November and have similar general meteorological conditions. We show the correlation coefficient and the coefficient of determination for both case and all the LWP bin. We observe a higher correlation of aerosol concentration and cloud properties in the lower values of LWP (from 30 to $70\,g\,m^{-2}$). This suggests that aerosol–cloud interactions are a more significant process at the lower LWP and when it get to higher values, other processes such as collision and coalescence are a dominant cloud microphysical process. This can be further explained by an occurrence of drizzle close to cloud base when the values of LWP are above $75\,g\,m^{-2}$. We also observed an increase of the correlation between

AMTD
8, 11953–11986, 2015

the aerosol and cloud properties when the parameters are compared at a set height dependent on the cloud base height.

The method we developed is based on a synergy of widely available, high resolution remote sensing instruments. It enables monitoring the interactions of aerosols and clouds. Although the data needs to comply with restrictive criteria, the use of a Cloudnet data format and the categorisation product makes data selection possible in close to real-time. We showed that using the integrated value of the attenuated backscatter from lidar enables the monitoring of aerosol–cloud interactions. The measurements from radar, lidar and microwave radiometer are collected continuously and can therefore provide a continuous estimate of effects of aerosol concentration on cloud properties. This framework of measurements can be implemented at any observatory where the Cloudnet dataset is available and can be integrated into a Cloudnet framework as one of the products. The software developed for this methodology is available under GNU General Public License (Sarna, 2015). Monitoring aerosol–cloud interactions in the same manner over multiple regions will allow for more studies of these phenomena and will result in a better understanding of the interactions between aerosol and clouds.

Acknowledgements. The research leading to these results has received funding from the European Union Seventh Framework Programme (FP7/2007-2013) under grant agreement 262254.

We acknowledge the Cloudnet project (European Union contract EVK2-2000-00611) for providing the Cloudnet Target Categorisation dataset, which was produced by the Department of Meteorology from the University of Reading using measurements from the US Department of Energy as part of the Atmospheric Radiation Measurement (ARM) Mobile Facility (AMF) Climate Research Facility at Graciosa, Azores.

The authors would like to acknowledge Christine Knist and thank her for providing the cloud microphysical properties dataset used in this study.

AMTD
8, 11953–11986, 2015

References

Brenguier, J.-L., Burnet, F., and Geoffroy, O.: Cloud optical thickness and liquid water path – does the *k* coefficient vary with droplet concentration?, Atmos. Chem. Phys., 11, 9771–9786, doi:10.5194/acp-11-9771-2011, 2011. 11963

Draxler, R. R. and Hess, G. D.: Description of the HYSPLIT-4 Modeling System, National Oceanic and Atmospheric Administration, Silver Spring, MD, USA, 1997. 11965

Feingold, G.: Modeling of the first indirect effect: analysis of measurement requirements, Geophys. Res. Lett., 30, 1997, doi:10.1029/2003GL017967, 2003. 11955, 11960, 11968

Feingold, G., Remer, L. A., Ramaprasad, J., and Kaufman, Y. J.: Analysis of smoke impact on clouds in Brazilian biomass burning regions: an extension of Twomey's approach, J. Geophys. Res., 106, 22907–22922, doi:10.1029/2001JD000732, 2001. 11957

Feingold, G., Eberhard, W. L., Veron, D. E., and Previdi, M.: First measurements of the Twomey indirect effect using ground-based remote sensors, Geophys. Res. Lett., 30, 1287, doi:10.1029/2002GL016633, 2003. 11964

Feingold, G., Furrer, R., Pilewskie, P., Remer, L. A., Min, Q., and Jonsson, H.: Aerosol indirect effect studies at Southern Great Plains during the May 2003 Intensive Operations Period, J. Geophys. Res., 111, D05S14, doi:10.1029/2004JD005648, 2006. 11961, 11964

Frisch, S., Shupe, M., Djalalova, I., Feingold, G., and Poellot, M.: The retrieval of stratus cloud droplet effective radius with cloud radars, J. Atmos. Ocean. Tech., 19, 835–842, doi:10.1175/1520-0426(2002)019<0835:TROSCD>2.0.CO;2, 2002. 11962

Garrett, T. J., Zhao, C., Dong, X., Mace, G. G., and Hobbs, P. V.: Effects of varying aerosol regimes on low-level Arctic stratus, Geophys. Res. Lett., 31, L17105, doi:10.1029/2004GL019928, 2004. 11955

Hogan, R. J. and O'Connor, E. J.: Facilitating cloud radar and lidar algorithms: the Cloudnet Instrument Synergy/Target Categorization product, CLOUDNET Project Documentation, Reading, UK, 2004. 11960, 11962

Illingworth, A. J., Hogan, R. J., O'Connor, E. J., Bouniol, D., Delanoë, J., Pelon, J., Protat, A., Brooks, M. E., Gaussiat, N., Wilson, D. R., Donovan, D. P., Baltink, H. K., van Zadelhoff, G.-J., Eastment, J. D., Goddard, J. W. F., Wrench, C. L., Haeffelin, M., Krasnov, O. A., Russchenberg, H. W. J., Piriou, J.-M., Vinit, F., Seifert, A., Tompkins, A. M., and Willén, U.: Cloudnet, B. Am. Meteorol. Soc., 88, 883–898, doi:10.1175/BAMS-88-6-883, 2007. 11955

AMTD
8, 11953–11986, 2015

IPCC (Ed.): Climate Change 2013 – The Physical Science Basis: Working Group I Contribution to the Fifth Assessment Report of the Intergovernmental Panel on Climate Change, Cambridge University Press, Cambridge, 2014. 11954

Kaufman, Y. J., Koren, I., Remer, L. A., Rosenfeld, D., and Rudich, Y.: The effect of smoke, dust, and pollution aerosol on shallow cloud development over the Atlantic Ocean, P. Natl. Acad. Sci. USA, 102, 11207–11212, doi:10.1073/pnas.0505191102, 2005. 11955

Kim, B.-G., Miller, M. A., Schwartz, S. E., Liu, Y., and Min, Q.: The role of adiabaticity in the aerosol first indirect effect, J. Geophys. Res., 113, D05210, doi:10.1029/2007JD008961, 2008. 11955

Knist, C. L.: Retrieval of liquid water cloud properties from ground-based remote sensing observations, PhD thesis, TU Delft, Civil Engineering and Geosciences, Geoscience and Remote Sensing, Delft, the Netherlands, 2014. 11962, 11963

Kovalev, V. A.: Solutions in LIDAR Profiling of the Atmosphere, John Wiley & Sons, Hoboken, NJ, USA, 2015. 11961

Köhler, H.: The nucleus in and the growth of hygroscopic droplets, T. Faraday Soc., 32, 1152–1161, doi:10.1039/TF9363201152, 1936. 11960

Lamb, D. and Verlinde, J.: Physics and Chemistry of Clouds, Cambridge University Press, Cambridge, UK, 2011. 11960

Lu, M.-L., Conant, W. C., Jonsson, H. H., Varutbangkul, V., Flagan, R. C., and Seinfeld, J. H.: The Marine Stratus/Stratocumulus Experiment (MASE): aerosol–cloud relationships in marine stratocumulus, J. Geophys. Res., 112, D10209, doi:10.1029/2006JD007985, 2007. 11960

Lu, M.-L., Feingold, G., Jonsson, H. H., Chuang, P. Y., Gates, H., Flagan, R. C., and Seinfeld, J. H.: Aerosol-cloud relationships in continental shallow cumulus, J. Geophys. Res., 113, D15201, doi:10.1029/2007JD009354, 2008. 11955

Martin, G. M., Johnson, D. W., and Spice, A.: The measurement and parameterization of effective radius of droplets in warm stratocumulus clouds, J. Atmos. Sci., 51, 1823–1842, doi:10.1175/1520-0469(1994)051<1823:TMAPOE>2.0.CO;2, 1994. 11960, 11966

McComiskey, A. and Feingold, G.: The scale problem in quantifying aerosol indirect effects, Atmos. Chem. Phys., 12, 1031–1049, doi:10.5194/acp-12-1031-2012, 2012. 11955

McComiskey, A., Feingold, G., Frisch, A. S., Turner, D. D., Miller, M. A., Chiu, J. C., Min, Q., and Ogren, J. A.: An assessment of aerosol–cloud interactions in marine stratus clouds based on

AMTD
8, 11953–11986, 2015

surface remote sensing, J. Geophys. Res., 114, D09203, doi:10.1029/2008JD011006, 2009. 11955
Münkel, C., Eresmaa, N., Räsänen, J., and Karppinen, A.: Retrieval of mixing height and dust concentration with lidar ceilometer, Bound.-Lay. Meteorol., 124, 117–128, doi:10.1007/s10546-006-9103-3, 2006. 11961
O'Connor, E. J., Illingworth, A. J., and Hogan, R. J.: A technique for autocalibration of cloud lidar, J. Atmos. Ocean. Tech., 21, 777–786, doi:10.1175/1520-0426(2004)021<0777:ATFAOC>2.0.CO;2, 2004. 11961
Pruppacher, H. R. and Klett, J. D.: Microphysics of Clouds and Precipitation, Springer, Dordrecht, Netherlands, 2010. 11956
Rémillard, J., Kollias, P., Luke, E., and Wood, R.: Marine boundary layer cloud observations in the Azores, J. Climate, 25, 7381–7398, doi:10.1175/JCLI-D-11-00610.1, 2012. 11965, 11967
Sarna, K.: ACI monitoring: first release, doi:10.5281/zenodo.32033, Computer Software, 2015. 11971
Stephens, G. L.: Radiation profiles in extended water clouds. II: Parameterization schemes, J. Atmos. Sci., 35, 2123–2132, doi:10.1175/1520-0469(1978)035<2123:RPIEWC>2.0.CO;2, 1978. 11957
Sundström, A.-M., Nousiainen, T., and Petäjä, T.: On the quantitative low-level aerosol measurements using ceilometer-type lidar, J. Atmos. Ocean. Tech., 26, 2340–2352, doi:10.1175/2009JTECHA1252.1, 2009. 11961
Turner, D. D., Vogelmann, A. M., Johnson, K., Miller, M., Austin, R. T., Barnard, J. C., Flynn, C., Long, C., McFarlane, S. A., Cady-Pereira, K., Clough, S. A., Chiu, J. C., Khaiyer, M. M., Liljegren, J., Lin, B., Minnis, P., Marshak, A., Matrosov, S. Y., Min, Q., O'Hirok, W., Wang, Z., and Wiscombe, W.: Thin liquid water clouds: their importance and our challenge, B. Am. Meteorol. Soc., 88, 177–190, doi:10.1175/BAMS-88-2-177, 2007. 11964
Twohy, C. H., Petters, M. D., Snider, J. R., Stevens, B., Tahnk, W., Wetzel, M., Russell, L., and Burnet, F.: Evaluation of the aerosol indirect effect in marine stratocumulus clouds: droplet number, size, liquid water path, and radiative impact, J. Geophys. Res., 110, D08203, doi:10.1029/2004JD005116, 2005. 11955
Twomey, S.: Pollution and the planetary albedo, Atmos. Environ., 8, 1251–1256, doi:10.1016/0004-6981(74)90004-3, 1974. 11954, 11956, 11957

AMTD
8, 11953–11986, 2015

Twomey, S.: The influence of pollution on the shortwave albedo of clouds, J. Atmos. Sci., 34, 1149–1152, doi:10.1175/1520-0469(1977)034<1149:TIOPOT>2.0.CO;2, 1977. 11956

Twomey, S. and Warner, J.: Comparison of measurements of cloud droplets and cloud nuclei, J. Atmos. Sci., 24, 702–703, doi:10.1175/1520-0469(1967)024<0702:COMOCD>2.0.CO;2, 1967. 11956, 11958

Widener, K. B. and Mead, J. B.: W-Band ARM cloud radar-Specifications and design, in: Fourteenth ARM Science Team Meeting Proceedings, Albuquerque, NM, USA, available at: http://www.arm.gov/publications/proceedings/conf14/extended_abs/widener2-kb.pdf, 2004. 11965

Wiegner, M., Madonna, F., Binietoglou, I., Forkel, R., Gasteiger, J., Geiß, A., Pappalardo, G., Schäfer, K., and Thomas, W.: What is the benefit of ceilometers for aerosol remote sensing? An answer from EARLINET, Atmos. Meas. Tech., 7, 1979–1997, doi:10.5194/amt-7-1979-2014, 2014. 11961

AMTD
8, 11953–11986, 2015

Table 1. Cloud and aerosol properties measured or derived from the observations at the Graciosa Island, Azores.

Measured Quantity	Definition	Instrument(s)
Cloud Liquid Water Path	LWP [$g\,m^{-2}$]	MWR
Radar Reflectivity Factor	Z [dBZ or $m^6\,m^{-3}$]	WACR
Cloud Droplet Effective Radius	r_e [µm] (see Eq. 7)	WACR/MWR
Cloud Droplets Number Concentration	N_d [cm^{-3}] (see Eq. 8)	WACR/MWR
Attenuated Backscatter Coefficient	ATB [$m^{-1}\,sr^{-1}$]	Vaisala CT25K

AMTD
8, 11953–11986, 2015

Table 2. The statistical parameters calculated between ln(r_e) and ln(ATB), namely Pearson Product–Moment Correlation Coefficient, r, and the Coefficient of Determination, r^2 and the number of observations within the LWP bins, n, for two study cases from Graciosa Island at the Azores (3 and 29 November 2009).

	3 November 2009			29 November 2009		
LWP bin	r	r^2	n	r	r^2	n
30 < LWP < 40	−0.76	0.58	71	−0.36	0.13	54
40 < LWP < 50	−0.80	0.65	43	−0.56	0.32	63
50 < LWP < 60	−0.70	0.49	56	−0.68	0.47	67
60 < LWP < 70	−0.50	0.25	95	−0.64	0.41	98
70 < LWP < 80	−0.33	0.11	62	−0.31	0.10	98
80 < LWP < 90	−0.27	0.07	44	0.57	0.32	39
90 < LWP < 100	−0.53	0.28	16	–	–	–
100 < LWP < 110	−0.47	0.22	8	–	–	–

AMTD
8, 11953–11986, 2015

Table 3. The statistical parameters calculated between ln(N_d) and ln(ATB), namely the Pearson Product–Moment Correlation Coefficient, r, and the Coefficient of Determination, r^2 and the number of observations, n, for two study cases from Graciosa Island at the Azores (3 and 29 November 2009).

3 November 2009			29 November 2009		
r	r^2	n	r	r^2	n
0.57	0.33	395	0.40	0.16	419

AMTD
8, 11953–11986, 2015

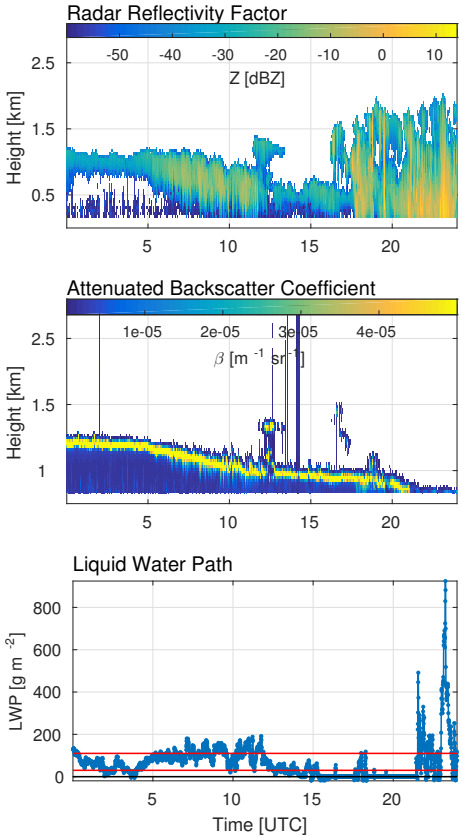

Figure 1. The time-height cross section of the Radar Reflectivity Factor from WACR, the Attenuated Backscatter Coefficient from Vaisala CT25K and the Liquid Water Path from MWR for a full day of measurements on 3 November 2009.

AMTD
8, 11953–11986, 2015

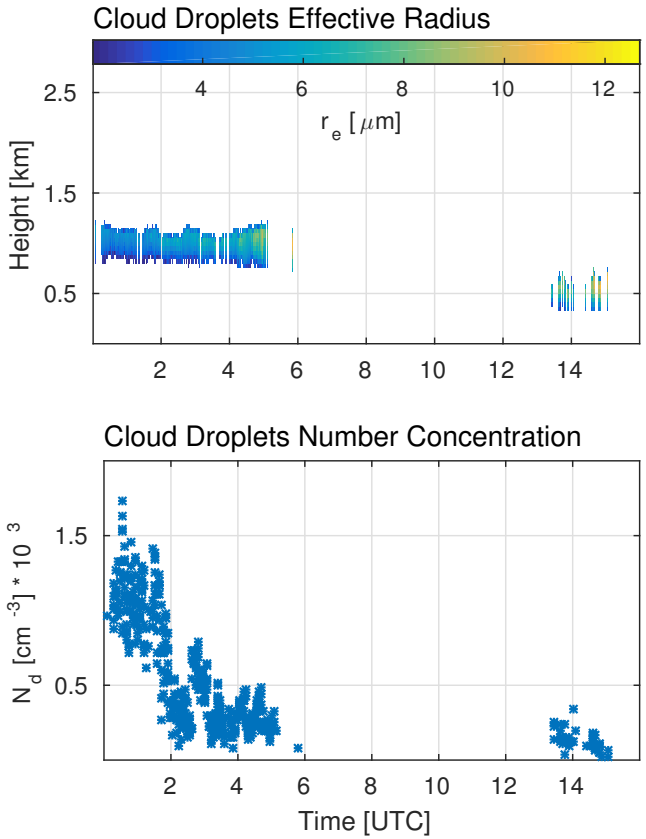

Figure 2. The time-height cross section of the Cloud Droplet Effective Radius (r_e) calculated from WACR and MWR measurements (Eq. 7) and the Cloud Droplet Number Concentration (N_d) calculated from Eq. (8) from 3 November 2009. Data is only retrieved in the time steps when the data selection criteria are met.

AMTD
8, 11953–11986, 2015

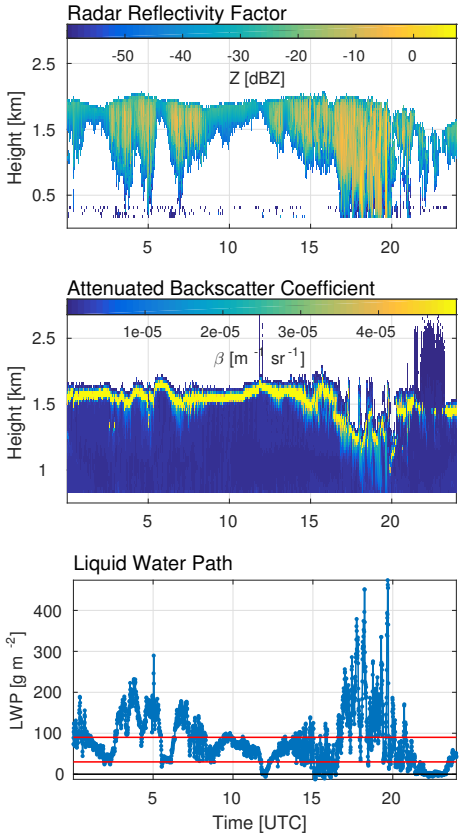

Figure 3. The time-height cross section of the Radar Reflectivity from WACR, the Attenuated Backscatter Coefficient from Vaisala CT25K and the Liquid Water Path from MWR for a full day of measurements on 29 November 2009.

AMTD
8, 11953–11986, 2015

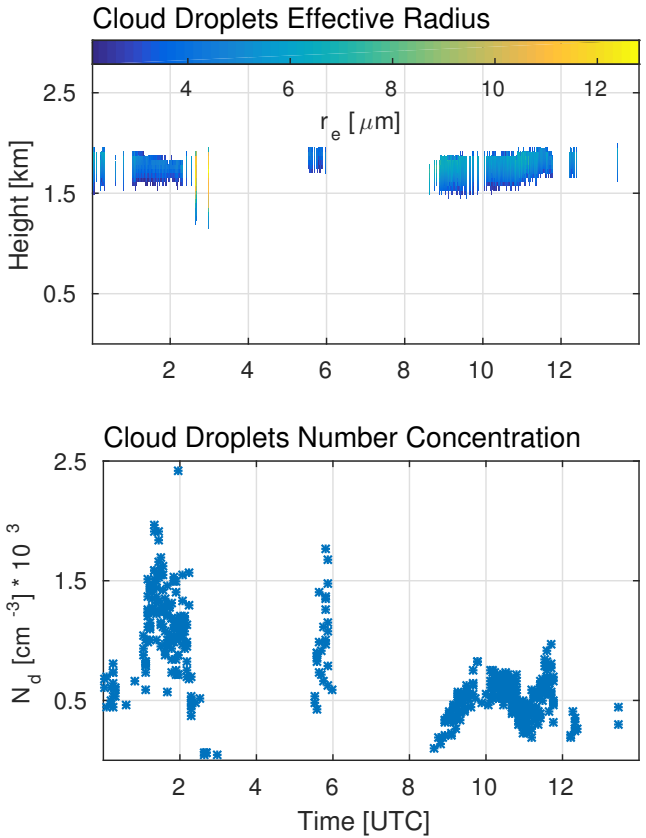

Figure 4. The time-height cross section of the Cloud Droplet Effective Radius (r_e) derived from the WACR and MWR (Eq. 7) and the Cloud Droplet Number Concentration (N_d) calculated from Eq. (8) from 29 November 2009. Data is only retrieved in the time steps when the data selection criteria are met.

AMTD
8, 11953–11986, 2015

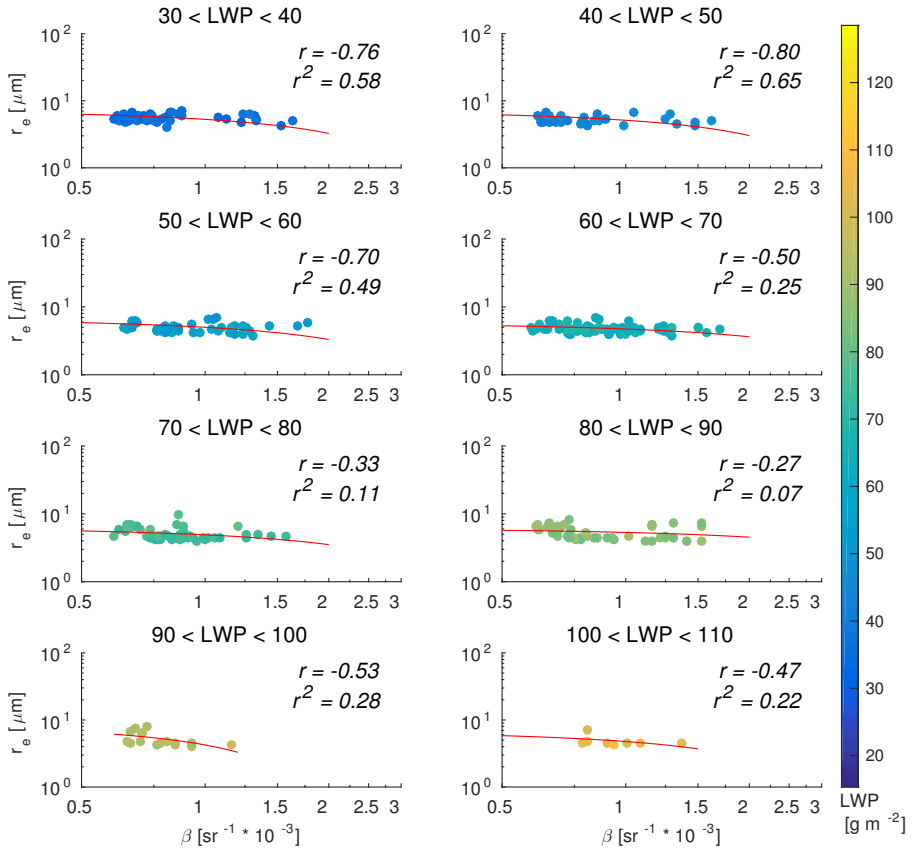

Figure 5. The values of the effective radius r_e derived from WACR and MWR measurements are plotted vs. the integrated attenuated backscatter ATB measured by Vaisala CT25K on 3 November 2009. Data are sorted by the values of LWP from MWR. Every panel shows the corresponding value of the Pearson Product–Moment Correlation Coefficient, r, and the Coefficient of Determination, r^2 and the regression line (red) for that LWP bin.

AMTD
8, 11953–11986, 2015

Monitoring aerosol–cloud interactions

K. Sarna and
H. W. J. Russchenberg

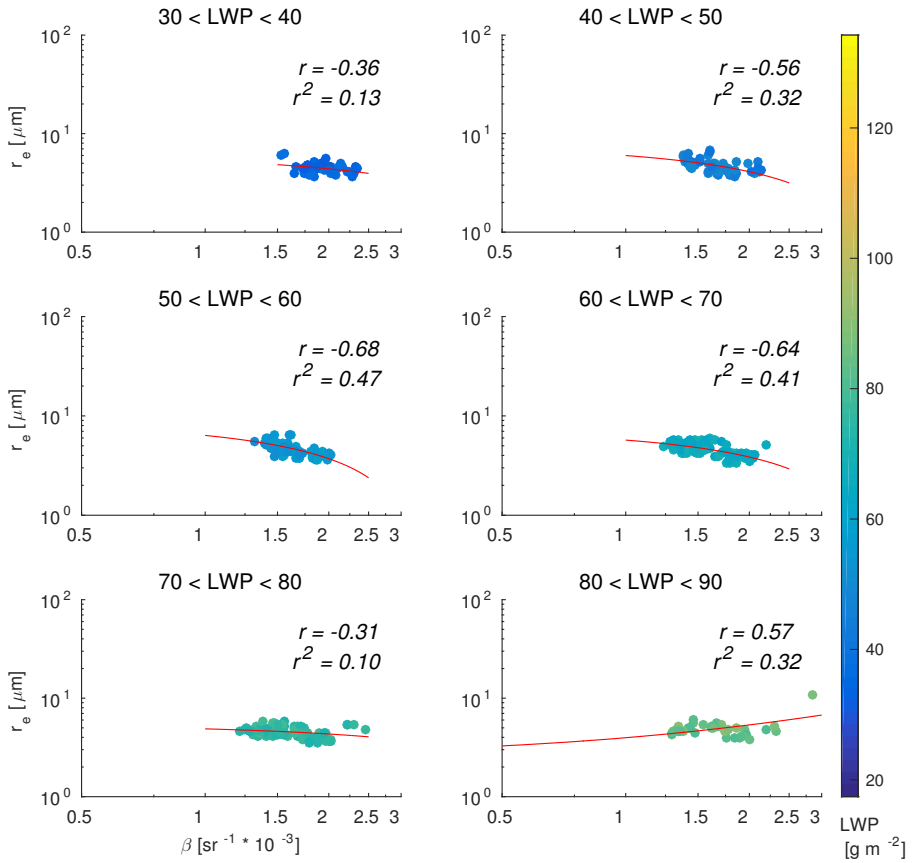

Figure 6. The values of the effective radius r_e derived from WACR and MWR measurements are plotted vs. the integrated attenuated backscatter ATB measured by Vaisala CT25K on 29 November 2009. Data are sorted by the values of LWP from MWR. Every panel shows the corresponding value of the Pearson Product–Moment Correlation Coefficient, r, and the Coefficient of Determination, r^2 and the regression line (red) for that LWP bin.

AMTD
8, 11953–11986, 2015

Monitoring aerosol–cloud interactions

K. Sarna and
H. W. J. Russchenberg

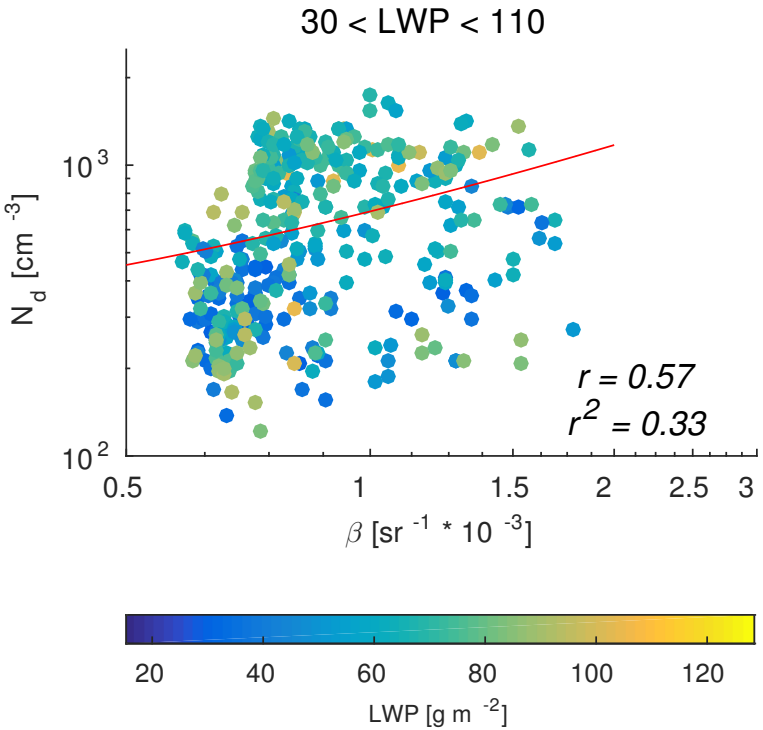

Figure 7. The cloud droplet number concentration N_d derived from WACR and MWR measurements with Eq. (8) is plotted vs. the integrated attenuated backscatter ATB measured by Vaisala CT25K on 3 November 2009. Corresponding value of the Pearson Product–Moment Correlation Coefficient, *r*, and the Coefficient of Determination, r^2 and the regression line (red) is presented.

AMTD
8, 11953–11986, 2015

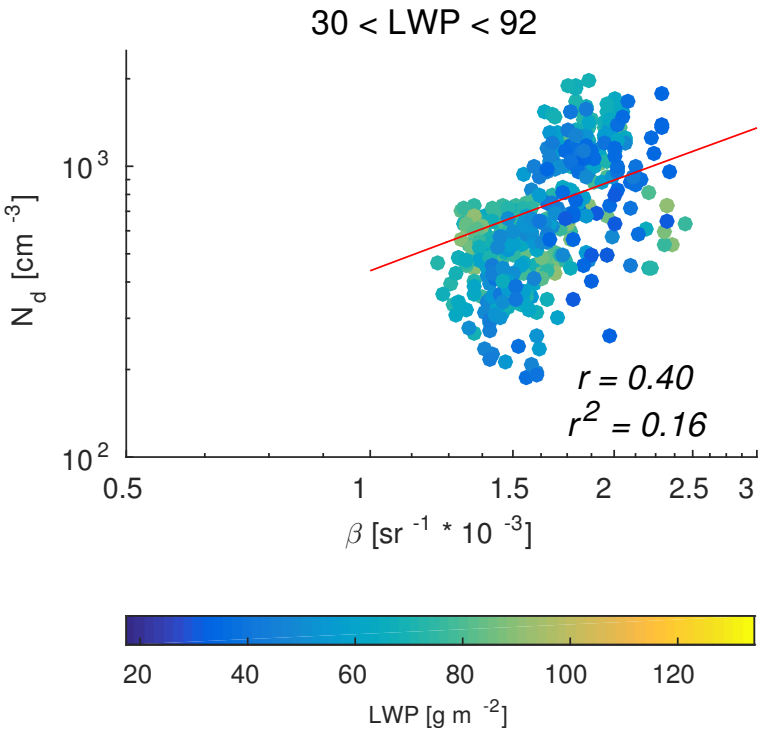

Figure 8. The cloud droplet number concentration N_d derived from WACR and MWR measurements with Eq. (8) is plotted vs. the integrated attenuated backscatter ATB measured by Vaisala CT25K on 29 November 2009. Corresponding value of the Pearson Product–Moment Correlation Coefficient, *r*, and the Coefficient of Determination, r^2 and the regression line (red) is presented.

AMTD
8, 11953–11986, 2015